Torque Ripple Reduction for PMSM based on PWM Pulse Merging Method for High Speed Range

Shona Noguchi, Hiroshi Fujimoto
The University of Tokyo
5-1-5, Kashiwanoha, Kashiwa, Chiba, 277-8561, Japan
Phone: +81-4-7136-3881
Email: noguchi.shona19@ae.k.u-tokyo.ac.jp, fujimoto@k.u-tokyo.ac.jp

***Abstract*—Permanent magnet synchronous motors (PMSMs) are widely used because of their high efficiency and lower energy consumption. However, the motor noise and the vibration caused by the torque ripple is a well-known problem because of an imperfect sinusoidal flux distribution. To reduce the torque ripple, the current controller based on the perfect tracking control (PTC) is reported. Although it has improved the tracking performance of a current reference compared to the proportional-integral (PI) feedback control and the suppression effect, there is still room for improvement of the current control by reference value oversampling. Thus, we have proposed the pulse merging method that samples a reference value twice more than the conventional method to improve the current control and applied it to the torque ripple suppression at the high-speed range. The proposed method could suppress the torque ripple more than the PTC from the simulation results.**

***Index Terms*—permanent magnet synchronous motor (PMSM), current control, perfect tracking control, torque ripple**

I. Introduction

Permanent magnet synchronous motors (PMSMs) are widely used for industrial applications. It is because PMSMs can be driven at high efficiency and by lower energy consumption. Especially interior permanent magnet synchronous motors (IPMSMs) are suitable for the use that demands high-efficiency and high-speed drive. However, the torque ripple is a well-known problem to emit the motor noise and the vibration. They can affect the other systems, so the torque ripple should be suppressed. There are two approaches to reduce the torque ripple. One is the mechanical approach. Especially the skew is the well-known method [1]. There are disadvantages in the processing cost and the reduction of the torque output though it is a simple way to reduce the torque ripple. On the other hand, control approaches have no such disadvantages because additional processing is not necessary. Therefore, a control approach is applied to reduce the torque ripple in this study. The proportional-integral (PI) feedback control is commonly used as a current control for motors. Several papers have reported that the torque ripple is reduced with the PI control [2]–[4]. It is also reported that the torque ripple has been suppressed by the feedforward controller based on the perfect tracking control (PTC) [5], [6]. A problem with the PI control is that when the reference value is steeply changed, the output current can not follow it. Therefore, the current controller to reduce the torque ripple is designed with a feedforward controller because it is necessary to guarantee the tracking performance of the reference value to drive motors at high speeds. Although the PTC has improved the tracking performance, there is still room for improvement. It is reported that the tracking performance has improved by the quasi multirate feedforward control whose sampling period of the reference value is twice more than the conventional method at the high-bandwidth [7] by the use of the PTC and the quasi multirate deadbeat control [8]. This method has improved under the condition of the same carrier frequency. Thus, we propose the new feedforward current controller that samples a reference value twice more than the PTC without changing the carrier frequency. The proposed method is designed in a single-rate system to guarantee the reference value tracking performance at a high-speed range. We also verified the torque ripple reduction effect in high-speed range with the use of the proposed method by the simulation.

In this study, the authors aim to reduce the torque ripple of the IPMSM by the PTC and PWM pulse merging methods. This paper is organized as follows: First, the control method is explained in Section Ⅱ; the setup of the simulation and its result are discussed in Section Ⅲ; finally, the conclusion is presented in Section Ⅳ.

II. Control Method

A. Perfect Tracking Control (PTC)

The control system based on the PTC can follow a reference trajectory without errors at every sampling point [9], [10]. It has been reported that this effect was achieved with a multirate controller [11]. This control system is two degrees of freedom control composed of a feedforward and a feedback controller. Disturbances and modeling errors are suppressed by a feedback controller in this control system. With using the time t in the continuous-time, there are two samplers for a reference $r(t)$ and an output signal $y(t)$, and one holder for an input $u(t)$, in a digital control system. Then, sampling parameters of sampling periods of $r(t)$, $y(t)$, and $u(t)$ are notated as T_r, T_y, and T_u, respectively.

B. PWM Hold Model

The model is considered as a single-phase inverter system

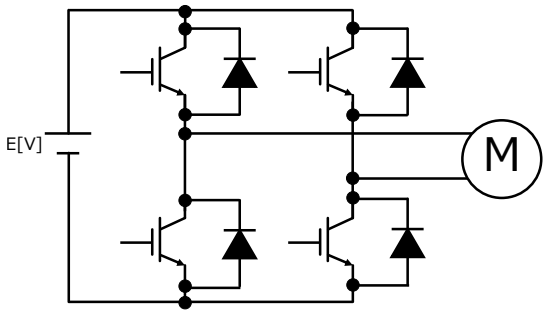

Fig. 1. Circuit diagram of single phase inverter

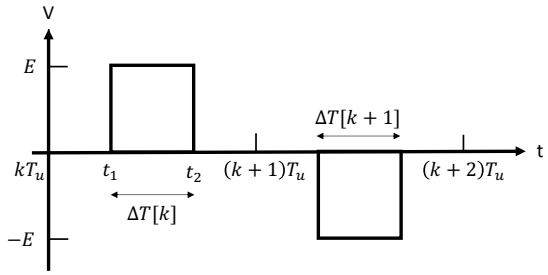

Fig. 2. Output of single phase inverter

shown in Fig. 1 to simplify the derivation of the holding model. The output from this inverter is either 0 V or $\pm E$ V as shown in Fig. 2. The discretization methods are shown in Fig. 3. In general, a zero-order hold (ZOH) is applied to discretize a control system. k is defined as sampling points at every carrier period. The control input $u[k]$ discretized by the ZOH is $V[k]$ at a sampling point k. However, it can be a more exact plant model compared to the ZOH to treat the pulse width as a control input. A pulse width modulation (PWM) hold is introduced in [12]. A control input $u[k]$ is obtained by discretizing a control system with an ON time $\Delta T[k]$. The state-space model (1) and (2) can be described by the PWM hold as follows:

$$\boldsymbol{x}[k+1] = \boldsymbol{A}_s\boldsymbol{x}[k] + \boldsymbol{b}_s\Delta T[k], \tag{1}$$

$$y[k] = \boldsymbol{c}_s\boldsymbol{x}[k], \tag{2}$$

where $\boldsymbol{A}_s = e^{\boldsymbol{A}_c T_u}$, $\boldsymbol{b}_s = e^{\boldsymbol{A}_c T_u/2}\boldsymbol{b}_c E$, $\boldsymbol{c}_s = \boldsymbol{c}_c$ and if $\Delta T < 0$, then the output voltage will be $-E$. This model is considered as a single-phase model, so if this model is applied to the three-phase model, it is necessary to convert to the three-phase model with the use of the method in [13].

C. Pulse Merging Method

The method to merge two adjacent PWM pulses is described in this subsection. Although a new control input can be described by simply adding PWM pulses as same as the quasi multirate feedforward control method [7], the method to merge PWM pulses into one pulse by the mathematical strict model is applied in this paper. An IPMSM plant model

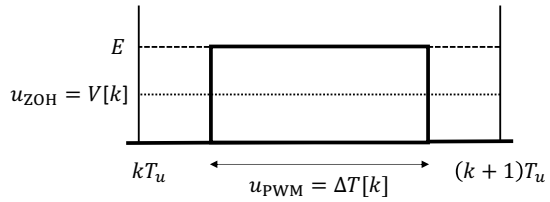

Fig. 3. DC voltage waveform discretized by ZOH and PWM hold

without considering the back EMF feedback loop $1/(Ls+R)$ is controlled and therefore the control system is designed as a single-rate system. The mathematical strict model to move a PWM pulse is described by the equation below [14]:

$$x[k+1] = e^{A_c T_u}x[k] + \int_{p_k^-}^{p_k^+} e^{A_c(T_u-\tau)}b_c E d\tau. \tag{3}$$

Here, $p_k^{\pm} = (T_u + 2h_k \pm \Delta T)/2$ and h_k is the offset from a center between sampling points $(k+1/2)T_u$ to a center of a PWM pulse. Fig. 4 and Fig. 5 show the PWM pulses after moving to the right end and the left end, respectively. The proposed method samples twice more than the conventional method and therefore a new pulse corresponds to the carrier frequency can be made by merging pulses. With using (3), the new control inputs are described based on the PTC [11] as below, respectively.

$$u_{\mathrm{R}}[k] = B_{\mathrm{R}}^{-1}(1 - z_s^{-1}A_{\mathrm{R}})x_d[k+1/2], \tag{4}$$

$$u_{\mathrm{L}}[k] = B_{\mathrm{L}}^{-1}(1 - z_s^{-1}A_{\mathrm{L}})x_d[k+1/2]. \tag{5}$$

Here, $A_{\mathrm{R}} = A_{\mathrm{L}} = e^{A_c T_u/2}$, $B_{\mathrm{R}} = b_c E$, $B_{\mathrm{L}} = e^{A_c T_u/2}b_c E$ and $z_s = e^{sT_u/2}$. x_d is a sampled reference value at every $T_u/2$. In case of $u_{\mathrm{R}}[k]$, p_k^+ and p_k^- are T_u and $T_u - \Delta T$, respectively. In case of $u_{\mathrm{L}}[k]$, p_k^+ and p_k^- are ΔT and 0, respectively. Considering the oversampling, the feedforward input calculation is held every half of the carrier period $T_u/2$. From (4) and (5), a new control input $u[k]$ is described as the addition of the two pulses to generate one pulse.

$$u[k] = u_{\mathrm{R}}[k] + u_{\mathrm{L}}[k+1/2]. \tag{6}$$

Thus, a new pulse is generated by merging two pulses as shown in Fig. 6. $u_{\mathrm{R}}[k]$ is not the as same value $u_{\mathrm{L}}[k+1/2]$ and therefore the center of a PWM pulse generated by a new control input $u[k]$ does not come to the center of the sample points of a reference $(k+1/2)T_u$. Then, $T_{\mathrm{shift}}[k]$ is introduced to treat the offset. The definition of $T_{\mathrm{shift}}[k]$ is shown in Fig. 7 and is described below:

$$T_{\mathrm{shift}}[k] = \frac{1}{2}(u_{\mathrm{R}}[k] - u_{\mathrm{L}}[k+1/2]). \tag{7}$$

If $T_{\mathrm{shift}}[k] > 0$, then an output pulse moves to the left. If $T_{\mathrm{shift}}[k] < 0$, then an output pulse moves to the right. The direction of a merged pulse is always calculated by (7) in this study. Thus, the control is performed by ON time that is moved to the right or left from the center of a PWM pulse. This effect in the current control is shown in Fig. 8. The current reference in this example simulation is the amplitude 1 A and

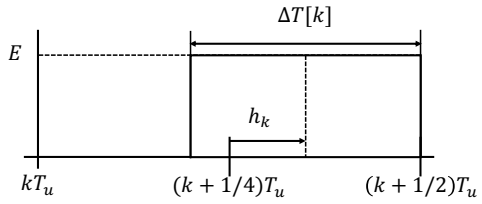

Fig. 4. PWM pulse moved to right end

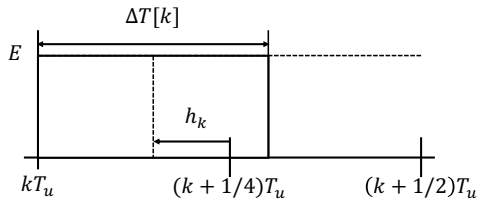

Fig. 5. PWM pulse moved to left end

2.5 kHz sine wave. From Fig. 8, the output PWM pulses of the proposed current controller do not match the center point between the sampling point of the reference value. The reference value tracking performance of the proposed method can be improved compared to the conventional single-rate PTC by oversampling of a reference and the degrees of freedom to shift the center position of a PWM pulse.

III. Simulation

A. Controller Design

Fig. 9 and Fig. 10 show the block diagrams in the simulation. S and H denote the sampler and the holder. respectively. Table I shows the parameters of the simulation. To reduce the torque ripple at a high-speed range, the pulse merging method is applied as the proposed feedforward controller in Fig. 10. Sampling periods of a reference value are noted as T_r in the conventional method and $T_r' = T_r/2$ in the proposed method. In this study, IPMSM is the controlled system, and its dq coordinate model is shown in Fig. 12. The d-axis current is determined based on the Maximum Torque Per Ampere (MTPA) control as below [15]:

$$i_d = \frac{K_e}{2(L_q - L_d)} - \sqrt{\frac{K_e^2}{4(L_q - L_d)^2} + i_q^2}. \tag{8}$$

From the calculation using the test motor parameters, the reference value i_d to drive at the maximum torque is approximately set to be 0 A because $\frac{K_e}{2(L_q - L_d)} \gg i_q$ in Table I.

The conventional feedforward controller is the PTC [11] and designed as follows. To simplify the analysis of the effect of the proposed method, the controllers designed by the dq-axis model. Since the transfer function from the voltage input to the current output does not consider the feedback loop due to the effect of the back EMF, the transfer function of the assumed plant model to design the feedforward controller is as below.

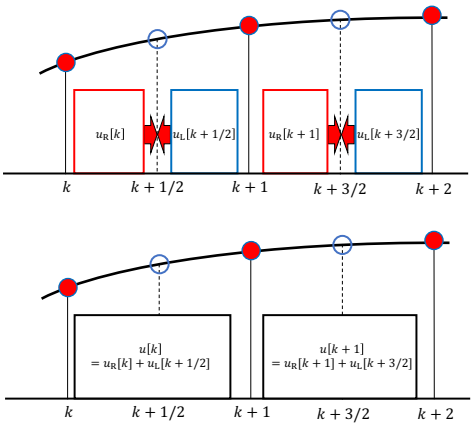

Fig. 6. Pulse merging method

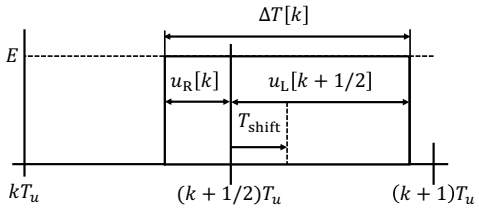

Fig. 7. Definition of T_{shift}

$$\frac{i}{v} = \frac{1}{Ls + R}. \tag{9}$$

The state space model of this model is described as follows with the state variable $x(t)$:

$$\dot{x}(t) = a_c x(t) + b_c u(t), \tag{10}$$

where $a_c = -\frac{R}{L}$ and $b_c = \frac{1}{L}$. Furthermore, the conventional feedforward controller is described by the transfer function of the plant (9) and then is substituted for (1)–(2) to determine the parameters in the discrete-time by the PWM hold. Finally, the control input $u[k]$ is described as follows by considering the stable inverse model of the plant model (9) to achieve PTC.

$$u[k] = b^{-1}(1 - z^{-1}a)x_d[k+1], \tag{11}$$

where $a = e^{-\frac{R}{L}T_u}$, $b = e^{-\frac{R}{L}\frac{T_u}{2}}\frac{1}{L}E$ and $z = e^{sT_r}$. This guarantees the perfect tracking of the nominal plant at every period of T_r. In the same way, a_R, b_R, a_L, b_L matrices of the proposed method are determined by (4)–(5). With considering oversampling, the discretization period is half of carrier frequency $T_u/2$. Here, $a_R = a_L = e^{-\frac{R}{L}\frac{T_u}{2}}$, $b_R = \frac{1}{L}E$, $b_L = e^{-\frac{R}{L}\frac{T_u}{2}}\frac{1}{L}E$. $P[z]$ in Fig. 9 and Fig. 10 is described by the PWM hold model of the plant. The current feedback controller C_{PI} is designed as a PI controller. The transfer function of the PI feedback controller is designed as follows.

$$C_{PI} = \frac{Ls + R}{\tau s}. \tag{12}$$

The controllers in the simulation are designed in discrete time using the Tustin transform by the sampling period T_u.

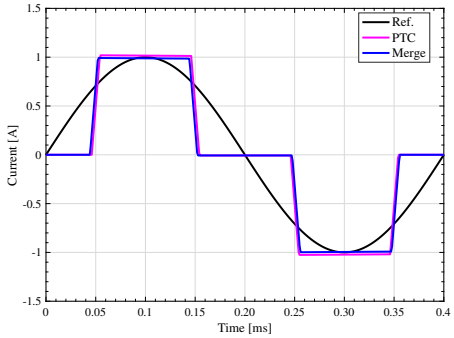

(a) q-axis current

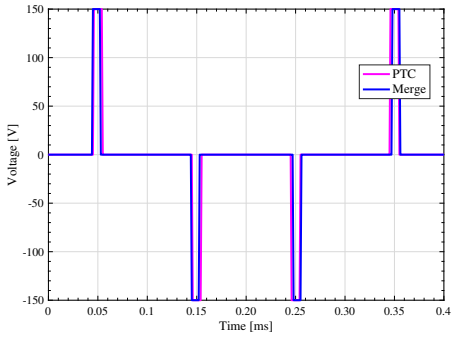

(b) q-axis PWM voltage

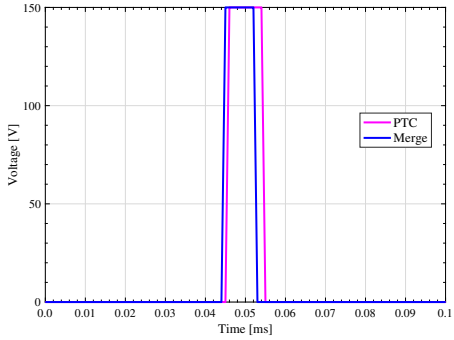

(c) q-axis PWM voltage (enlarged)

Fig. 8. Current control simulation

B. Torque Ripple Reduction

Fig. 13 shows the plant model in Fig. 9 and 10. The torque output considered with the ripple caused by the space harmonic is described below at dq-axis [16]:

$$\tau = P(\phi_d i_q - \phi_q i_d) \tag{13}$$

$$= P(K_{rt} i_d i_q + K_e i_q) + T_{rh}, \tag{14}$$

$$K_{rt} = (L_d - L_q), \tag{15}$$

$$T_{rh} = P(K_{hd} i_q \cos(6\theta_e) - K_{hq} i_d \sin(6\theta_e)). \tag{16}$$

T_{rh} is defined as a 6th order torque ripple caused by the space harmonic. The back EMF component caused by the space harmonic K_{hd} and K_{hq} is described below:

$$K_{hd} = K_{e5} + K_{e7}, \tag{17}$$

$$K_{hq} = -K_{e5} + K_{e7}. \tag{18}$$

Table. I
SIMULATION PARAMETERS OF TEST BENCH (FIG. 11)

Parameter	Value
Resistance R [$m\Omega$]	85.6
Inductance at d-axis L_d [mH]	0.613
Inductance at q-axis L_q [mH]	1.21
Pairs of poles P	6
Induced voltage constant K_e [V · s/rad]	0.0447
5th induced voltage constantK_{e5} [V · s/rad]	0.0041
7th induced voltage constantK_{e7} [mV · s/rad]	0.696
Torque constant K_t [N · m/A]	0.2679
Carrier frequency f_c [kHz]	10
Sampling period of reference T_r [μs]	100
Sampling period of output T_y [μs]	100
Control period T_u [μs]	100
DC input voltage of Inverter E [V]	150
Fundamental current reference i_{q0}^* [A]	7

Here, K_{e5} is the 5th induced voltage constant, and K_{e7} is the 5th induced voltage constant. The back EMF considered with the 6th order space harmonic is also defined with these parameters as below [16]:

$$e_q = \omega_e(K_e + K_{hd}\cos(6\theta_e)). \tag{19}$$

In the simulation, the torque ripple component T_{rh} described in the above is added at the torque output as shown in Fig. 13. The simulation is assumed that the decoupling control is perfectly achieved. Furthermore, it is assumed that the rotation speed is ideally controlled by the load motor. To suppress the torque ripple, the compensation component corresponds to the 6th harmonic is added to the reference current input i_{ref} in Fig. 9 and Fig. 10. The current reference i_{ref} is generated as below:

$$i_{\mathrm{ref}} = i_{q0}^* + \hat{A}_6 \sin(6\theta_e + \hat{\varphi}_6). \tag{20}$$

$\hat{A}_6$ is the amplitude of the 6th torque ripple component obtained by the FFT analysis and $\hat{\varphi}_6$ is adjusted to be the inverse phase of the torque ripple.

C. Result

Simulation results are shown in Fig. 14, Fig. 15, and Table II. Fig. 14 and Fig. 15 show the torque waveform. The rotation speeds ω is set at $2000\,\mathrm{rpm}$ and $4167\,\mathrm{rpm}$ to become the 6th harmonic at $1200\,\mathrm{Hz}$ and $2500\,\mathrm{Hz}$, respectively. $4167\,\mathrm{rpm}$ is the speed that the 6th harmonic comes to half of the Nyquist frequency determined by the carrier frequency. The performance of the proposed PTC with the pulse merging is compared to one of the single-rate PTC. From Fig. 14 and 15, The torque ripple is notably observed without compensation because it cannot follow beyond the PI control band. Both methods can reduce the torque ripple from the results in Fig. 14 and 15. The proposed method demonstrated a better reduction effect than the conventional method as the amplitude is less than the conventional method from Fig. 14 (a) and Fig. 15 (a). Furthermore, results of Fig. 14 (b) (c) and Fig. 15 (b) (c) show the FFT calculation results. From Table II, both methods can successfully reduce the torque ripple generated by the 6th harmonic and the proposed method demonstrated a better reduction effect than the conventional method. Thus, it can be predicted from the simulation results that the proposed method can be used for a method to reduce the torque ripple.

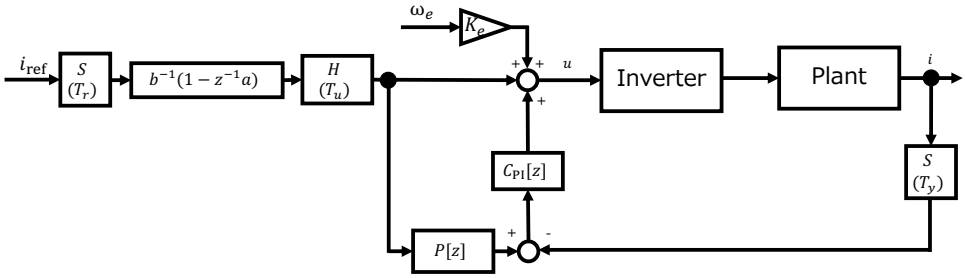

Fig. 9. Block diagram of conventional method in simulation ($z = e^{sT_u}$)

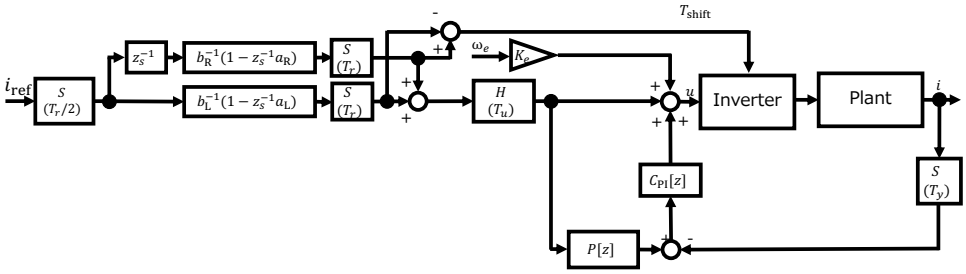

Fig. 10. Block diagram of proposed method in simulation ($z_s = e^{sT_u/2}$)

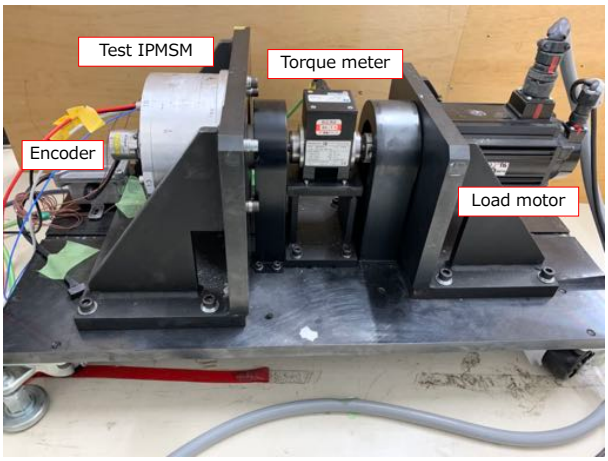

Fig. 11. Experimental setup

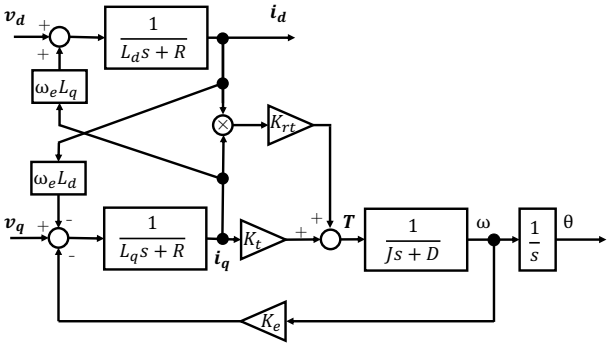

Fig. 12. Block diagram of IPMSM model with fundamental component at dq-axis

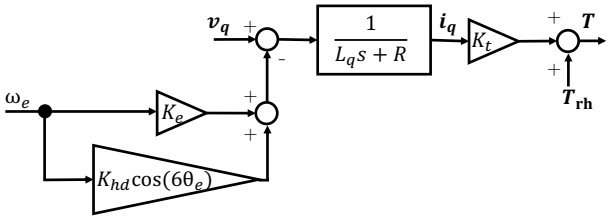

Fig. 13. Block diagram of simplified plant model with 6th harmonic component when $i_d = 0$ in simulation

IV. Conclusion

This paper proposes the torque ripple reduction method by the use of the PTC with the oversampling and the pulse merging at a high-speed range. The proposed method has been applied to the conventional feedforward control with the reference value oversampling and merging pulses in the single-rate system. Furthermore, The proposed method has the degree of freedom to shift a merged pulse from the center of sampling periods. The proposed method has demonstrated the torque ripple reduction effect compared to the conventional PTC by the simulation. However, this method is not verified by the experiment. Therefore, the future work will be 1) the experiential verification of the proposed method by our test bench shown in Fig. 11, and 2) the theoretical consideration and the optimization of T_{shift} that is simply calculated (7) in this paper.

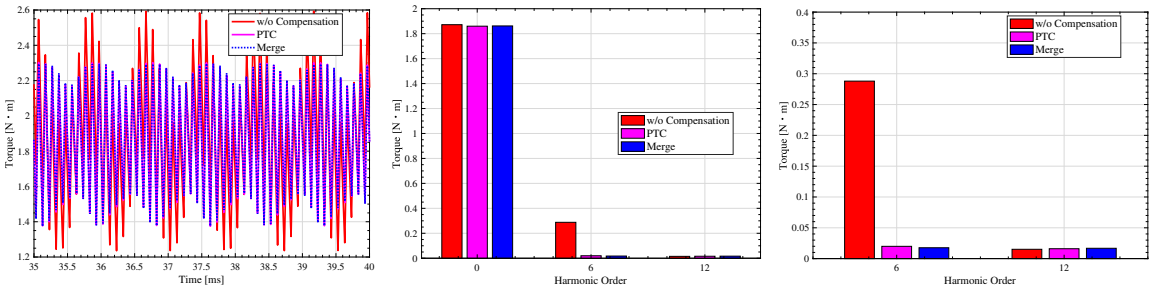

(a) Torque (b) Harmonic components (c) Harmonic components (enlarged)

Fig. 14. Simulation results of 6th harmonic torque ripple suppression ($\omega = 2000\,\mathrm{rpm}$)

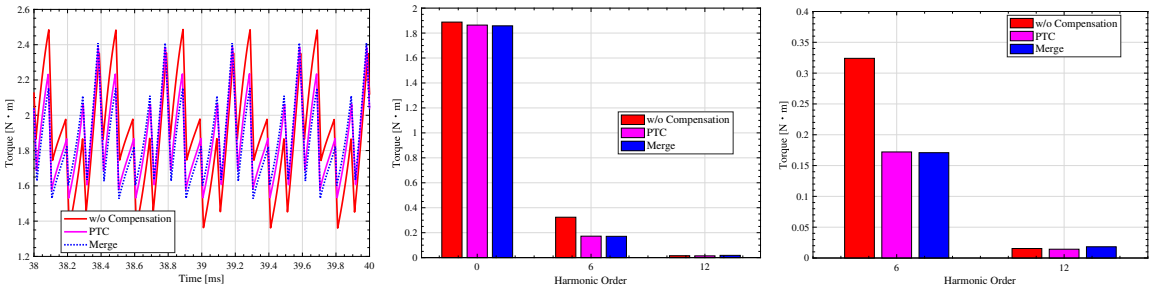

(a) Torque (b) Harmonic components (c) Harmonic components (enlarged)

Fig. 15. Simulation results of 6th harmonic torque ripple suppression ($\omega = 4167\,\mathrm{rpm}$)

Table. II
6TH HARMONIC OF TORQUE RIPPLE

Rotation speed [rpm]	Method	6th harmonic of torque ripple [N · m]
2000	w/o compensation	0.288
	PTC	0.0199
	Merge	0.0176
4167	w/o compensation	0.324
	PTC	0.172
	Merge	0.171

REFERENCES

[1] S. Morimoto and M. Sanada: "Principle and design of an energy saving motor", Kagaku Joho shuppan, Ibaraki(2013)(in Japanese)

[2] G. Feng, C. Lai and N. C. Kar: "Practical Testing Solutions to Optimal Stator Harmonic Current Design for PMSM Torque Ripple Minimization Using Speed Harmonics", IEEE Transaction on Power Electronics, Vol.33, No.6, pp. 5181-5191(2018)

[3] Y. Mao, S. Zuo, and J. Cao: "Effects of Rotor Position Error on Longitudinal Vibration of Electric Wheel System in In-Wheel PMSM Driven Vehicle", IEEE/ASME Transactions on Mechatronics, Vol.23, No.3, pp. 1314-1325(2018)

[4] L. Yan, Y. Liao, H. Lin and J. Sun: "Torque ripple suppression of permanent magnet synchronous machines by minimal harmonic current injection", IET Power Electronics, Vol.12, No.6, pp. 1368-1375(2019)

[5] K. Nakamura, H. Fujimoto and M. Fujitsuna, "Torque ripple suppression control for PM motor with high bandwidth torque meter," 2009 IEEE Energy Conversion Congress and Exposition, pp. 2572-2577(2009)

[6] K. Nakamura, H. Fujimoto and M. Fujitsuna, "Torque ripple suppression control for PM motor with current control based on PTC," The 2010 International Power Electronics Conference, pp. 1077-1082(2010)

[7] S. Noguchi, M. Mae and H. Fujimoto: "High-Bandwidth Current Control of PMSM Based on Quasi Multirate Feedforward Control", IEEJ International Workshop on Sensing, Actuation, Motion Control, and Optimization, (2020)

[8] R. Saito, K. Tsuchida and T. Yokoyama: "Digital Control of PWM Inverter Using Ultrahigh-Speed Network for Feedback Signals with Communication Disturbance Observer Based on Rocket I/O Protocol", IEEJ Journal of Industry Applications, Vol.4, No.6, pp. 752-757(2015)

[9] M. Tomizuka: "Zero Phase Error Tracking Algorithm for Digital Control," Journal of Dynamic Systems, Measurement, and Control, vol. 109, no. 1, pp. 65–68(1987)

[10] A. Kawamura, H. Fujimoto and T. Yokoyama, "Survey on the real time digital feedback control of PWM inverter and the extension to multi-rate sampling and FPGA based inverter control," IECON 2007 - 33rd Annual Conference of the IEEE Industrial Electronics Society, pp. 2044-2051(2007)

[11] H. Fujimoto, Y. Hori, A. Kawamura: "Perfect tracking control based on multirate feedforward control with generalized sampling periods", IEEE Trans. Industrial Electronics, vol. 48, No. 3, pp. 636–644(2001)

[12] K. P. Gokhale, A. Kawamura and R. G. Hoft: "Dead Beat Microprocessor Control of PWM Inverter for Sinusoidal Output Waveform Synthesis", IEEE Transactions on Industry Applications, Vol.23, no.3, pp. 901-910(1987)

[13] K. Sakata and H. Fujimoto: "Perfect Tracking Control of Servo Motor Based on Precise Model with PWM Hold and Current Loop", Power Conversion Conference, pp. 1077-1082(2007)

[14] M. Suzuki and M. Hirata: "Exact Linearization of PWM-Hold Discrete-Time Systems Using Input Transformation", European Control Conference, pp. 446-451(2015)

[15] Y. Takeda, N. Matsui, S. Morimoto and Y. Honda: "Design and Control for Interior Permanent Magnet Synchronous Motor", Ohmsha, Tokyo(2012)(in Japanese)

[16] N. Nakao, K. Tobari, T .Sugino, Y .Ito, M .Mishima and D .Maeda: "Minimizating Pulsating Torque in PMSM Drives by using Feedforward-based Compensation and Flux-harmonic Estimation", IEEE Energy Conversion Congress and Exposition, pp. 3030-3037(2020)